

Thermo-kinetic Computer Simulation of Differential Scanning Calorimetry Curves of AlMgSi Alloys

Ahmad Falahati¹, Erwin Povoden-Karadeniz², Peter Lang², Piotr Warczok¹, Ernst Kozeschnik^{1,2}

¹ Vienna University of Technology, Institute of Materials Science and Technology, Favoritenstr. 9-11/E308, 1040 Vienna, Austria

² Christian Doppler Laboratory "Early Stages of Precipitation", Vienna University of Technology, Institute of Materials Science and Technology, Vienna, Austria.

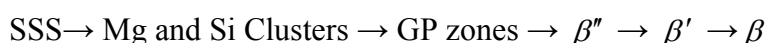
The microstructure evolution in heat-treatable Al-alloys is characterized by a complex sequence of precipitation processes. These can be either endothermic or exothermic in nature and they can be investigated by thermal analysis. The individual peaks identified in a differential scanning calorimetry (DSC) analysis can be attributed to the nucleation, growth and dissolution of certain types of precipitates. Simultaneously, these data can also be obtained by thermo-kinetic simulation based on models implemented, for instance, in the software MatCalc. The simulations make use of information stored in thermodynamic databases commonly used for equilibrium phase diagram calculations. Since thermodynamic information for metastable phases is generally lacking in these databases, in the present work, we show that these data can be obtained from the combination of experimental investigation with DSC, thermo-kinetic computational analysis and implementation of lattice stability data from ab-initio modeling. On the example of the Al-Mg-Si system, we demonstrate that the comparison between experimentally observed DSC signals for precipitation and dissolution of metastable GP-zones, β'' , β' , as well as stable β -Mg₂Si and Si precipitates with the kinetic simulation allows for an optimization of the thermodynamic data, particularly for the metastable phases. With the proposed methodology, consistent sets of parameters to describe the non-equilibrium thermodynamics and kinetics of complex systems can be obtained, which can finally aid in alloy and process development.

Keywords: AlMgSi; metastable phases; DSC; thermo-kinetic simulation; lattice stability.

1. Introduction

Aluminum alloys are important technological materials due to their advantageous strength-to-weight ratio, corrosion resistance and relatively low cost. One of the most important heat treatable Al alloy system is Al-Mg-Si (6xxx series). They are nowadays widely used for automotive body sheet due to their good hardenability, but also in part because of their good paint-baking response.

The considerable strength of Al-Mg-Si alloys is mainly due to a fine dispersion of particles precipitating from a supersaturated solid solution (SSS) after annealing and quenching. The generic precipitation sequence that is generally accepted for Al-Mg-Si- alloys is [1, 2]:



The only thermodynamically stable phase in the above sequence of precipitation is β , which is incoherent with the matrix. In most heat-treatable aluminum alloys, the thermodynamically stable phases are of only minor interest for industrial application, since the metastable phases contribute most to the mechanical properties.

In the present work, a computational tool for simulation of phase transformations based on CALPHAD-type multi-component thermodynamics [3, 4] is applied. Unfortunately, for the Al-system, even the comprehensive thermodynamic CALPHAD databases for light metals (e.g. the

COST database, or the commercially available Al-databases from ThermoCalc or ThermoTech are commonly missing the Gibbs energies of those metastable phases, which are particularly important in the present context. Recently, advanced methods have been pushed forward in the field of ab-initio modeling of phase stabilities, which can help to identify stable structures as well as provide part of the parameters required for precipitation simulations. Corresponding data has been implemented in a thermodynamic CALPHAD database including the free energies of the metastable phases of the Al-Mg-Si system [5, 6].

In this article, differential scanning calorimetry (DSC) is utilized to study non-isothermal precipitation sequences in the Al-Mg-Si system. The basis of non-isothermal DSC analysis is to measure the amount of energy absorbed (endothermic peaks) or released (exothermic peaks) by a well-defined sample during continuous heating or cooling in comparison to a given reference sample. The energy released or absorbed in this experiment can be directly related to the evolution of the volume fractions of transformed phases and the composition of the Al-matrix. Comparison between the experimental data and simulation results finally allows for the verification and optimization of the thermodynamic and kinetic parameters entering the simulations. This procedure is described in detail subsequently.

2. Thermo-kinetic computational analysis

In this section, the main ingredients for the computational analysis of precipitation and heat flux evolution during DSC probing are outlined.

2.1 Thermo-kinetic model

The evolution of precipitates of different phases in a solid-state system can be described by the sequence of nucleation, growth and coarsening. In the present work, the software MatCalc [7] (version 5.32) is used with the corresponding thermodynamic [mc_al_v0.10_2010-02-26] and mobility databases [mc_al_v1.03.ddb] for Al-alloys.

According to classical nucleation theory (CNT), the transient nucleation rate J can be written as in Eq.1.

$$J = N_0 Z \beta^* \exp\left(-\frac{\Delta G^*}{kT}\right) \exp\left(-\frac{\tau}{t}\right) \quad (1),$$

where N_0 is the number of potential nucleation sites, Z is the Zeldovich-factor, β^* is the atomic rate of attachment to the critical nucleus, ΔG^* is the Gibbs free energy of forming a critical nucleus, k the Boltzmann constant and T the absolute temperature. The Zeldovich factor Z is dimensionless and is related to the observation that thermal vibrations destabilize the nucleus as compared to the inactivated state. The incubation time τ is approximately the amount of time before particles reach the critical size and is determined by factors such as atomic mobility, driving force, interfacial energy etc. The total number of newly nucleated precipitates, which is an important characteristic quantity of a kinetic system, can be reasonably well calculated by Eq. 1 [8].

The further evolution of the supercritical nuclei is calculated with a model for the size and composition evolution of precipitates in multi-component, multi-phase systems as implemented in the MatCalc software [9].

2.2 Stable and metastable phases

From the generic precipitation sequence in Al-Mg-Si, the metastable GP-zone, β'' (Mg_5Si_6) and β' ($\text{Mg}_{1.8}\text{Si}$) precipitates, as well as the stable β (Mg_2Si) phase are included in the kinetic simulation. In 6xxx alloys with excess Si content above that ratio required to form stoichiometric Mg_2Si , Si precipitates in the stable diamond structure and is therefore included in the simulation. β and Si are the thermodynamically stable phases and they are accounted for in the simulations together

with the previously described metastable phases.

2.3 Interfacial energies

The interfacial energy between precipitate and matrix is a very sensitive input quantity for precipitation kinetics simulations. In the present work, the generalized n -nearest-neighbor broken-bond approach (GNB) is utilized as suggested recently by Sonderegger and Kozeschnik [10]. Since this quantity refers to the upper limit of the interfacial energy, corresponding to sharp and planar interfaces, the interfacial curvature and entropic effects at the interface and the effect of precipitate shape (spheres, platelets, needles,) is accounted by defining an additional correction factor with values below unity. The correction factors used in the simulations for the different precipitates are summarized in Table 1.

2.4 Lattice mismatch

The precipitates of the Al-Mg-Si system are characterized by a typical mismatch between the lattice parameter of the precipitate and the surrounding matrix. This misfit causes elastic stresses on precipitate growth, which can strongly affect the kinetics of precipitation. The energy contribution to the nucleation process coming from the volumetric misfit stresses is calculated according to reference [4].

If a precipitate nucleates in the bulk crystal, the entire misfit is theoretically operative in the nucleation process. In some cases, these values are reduced, however, due to the presence of excess vacancies, which aid to a fast relaxation of the ideal misfit stresses. For precipitates located at dislocations, we assume that a significant portion of the elastic misfit is compensated by either the compressive or tensile component of the dislocation stress field. The effective elastic misfit used in the simulations is therefore smaller than the value for homogeneous bulk nucleation. For precipitates nucleating at grain boundaries, we assume that there is no elastic misfit involved at all during nucleation, because all stresses are quickly relaxed by fast diffusion of vacancies and atoms along the grain boundaries and the incoherent phase boundaries[11].

There exists some uncertainty about the shape and lattice mismatch for GP-zones in Al-Mg-Si [12]. In the present work, we assume a volumetric mismatch of 1% for GP zone nucleation.

For β'' , first-principle calculations by Huis [2] indicate a lattice mismatch for different axes of 3.6, 0.6 and 5.3 %, respectively, with an angle difference of -5.2° . They correspond to a volumetric mismatch of 9.8%. Since β'' grows along the monoclinic b-axis in the direction of lowest lattice mismatch to minimize the coherency elastic strain part of its interfacial energy, a value of 2.0% is considered in the present analysis.

The β' -phase [13] is incoherent along the a- and b-axes. Because of incoherency and preferential nucleation at dislocations, no mismatch coherency elastic strain is considered for nucleation. The stable phases β and Si (in case of materials with excess Si) are incoherent with the matrix and are assumed to nucleate at dislocations. No effective lattice mismatch is considered for the nucleation of β , in contrast to a large volume mismatch for the Si diamond structure (19%) [14]. An effective mismatch of 5% in the early stages of precipitation is considered in the present study. The volumetric mismatch values considered here are summarized in Table 1.

2.5 Quenched-in vacancies

Since the diffusion kinetics in crystals is directly proportional to the density of vacant lattice sites [8], the amount of excess quenched-in vacancies and its time and temperature dependent evolution play a fundamental role in the early stages of precipitation [15]. During partial annihilation of excess quenched-in vacancies at dislocations, grain boundaries or incoherent phase boundaries, the chemical species exhibit significantly enhanced diffusional transport, thus contributing to early clustering and room temperature GP-zones formation.

Additionally, solute atoms with large size mismatch relieve the associated strain energy by pairing with vacancies or other solute atoms, resulting in the trapping of vacancies at clusters. The trapped vacancies can be released again in part during dissolution of the early clusters or GP-zones.

Vacancies that are released back into the still supersaturated matrix again facilitate ageing especially at low temperature. Both processes, the annihilation of quenched-in vacancies and the release of trapped vacancies are implemented in the software MatCalc. The excess quenched-in vacancies interaction with precipitates is associated in the model with the precipitate volume fraction that can effectively annihilate excess vacancies. The trapped vacancy release rate is also related to the precipitate volume fraction. For GP-zones, values of 0.02 and 0.00083 are used for these quantities.

2.6 Aluminum Matrix

The microstructural parameters of the matrix, grain size, subgrain size and dislocation density, depend on the manufacturing route and the thermo-mechanical history of the material. They will mainly affect the number of potential nucleation sites for the semi- and incoherent precipitates β' , β and Si nucleating at dislocations. In addition, they act as sources and sinks for vacancies and they define the mean diffusion distance for quenched-in vacancies to the next source and sink.

The elastic modulus of the aluminum matrix is an important input quantity for evaluation of the elastic misfit stress [4]. Its value is taken as $77.9 \cdot 10^9 - 7.3 \cdot 10^6 \cdot T$ [Pa] [6], where T is the temperature in Kelvin. Poisson's ratio for aluminum was taken as 0.3. A uniform dislocation density of $6 \cdot 10^{13} \text{ m}^{-2}$ has been assumed for the matrix.

Table 1: Volume mismatch, nucleation site and interfacial energy correction factor used in the simulations.

Phase	GP phase	β''	β'	β	Si
Coherency	Coherent	Coherent	Semi- coh.	Incoh.	Incoh.
Volume mismatch from literature (%)	2.6-5.8 [2]	9.8 [2]			19 [14]
Applied volume mismatch (%)	1	2			5
Nucleation sites	bulk	bulk	disl.	disl.	disl.
Interfacial energy correcting factor	0.7	0.87	0.92	1.0	1.0

3. Experimental

Specimens were taken from a commercial 6016 wrought Al-Mg-Si alloy 1.1 mm thick. The chemical composition of the alloys in wt% is Fe 0.19, Si 1.08, Cu 0.07, Mn 0.07, Mg 0.34, trace <0.02, balanced Al. In the simulations, we assume that Fe, Mn and Si form AlFeSi phases at rather high temperature. We further assume that these phases show no further reactions in the heat treatments, therefore, Fe and Mn are neglected in the simulations. The reduced composition of the 6016 is then Mg=0.35, Si=1.02 wt%. The effect of Cu is assumed to be minor in the present alloys.

The specimens were studied by light and scanning electron microscopy. The average grain size of the samples was approximately 100 μm . Subgrain size was estimated to be about 1 μm .

The DSC measurements were performed in a TA-Instrument DSC-2920 using a heating rate of 5 K/min in nitrogen atmosphere. DSC samples of 6mm diameter and 1mm thickness (~ 80 mg mass) were tested vs. 99.99 % pure-Al. Solution treatment was carried out at 540° for 30 minutes and then quenched in 25°C water. The freshly quenched samples were tested immediately.

4. Results and discussion

Figure 1 show a comparison between experimental and simulated DSC curves of the sample. The DSC signal shows four exothermic and two endothermic peaks. Sequentially, the peaks are assumed to be associated with cluster- and GP zones formation (A), dissolution of the GP zones (B), precipitation of β'' phase (C), precipitation of β' phase (D), precipitation of β and Si phases (E) and dissolution of β and Si phases (F).

Although the kinetics of precipitation peaks in DSC curves are complex, the sequence of simulated exo- and endothermic peaks are in complete agreement with experiments. The peak related to GP-zones and β'' simulations are almost identical as in the DSC experiment. The simulation peaks occur about the same temperature as the experiments.

Fig. 1: Comparison between experimental (symbols) and simulated (line) DSC curves of AA6016 sample

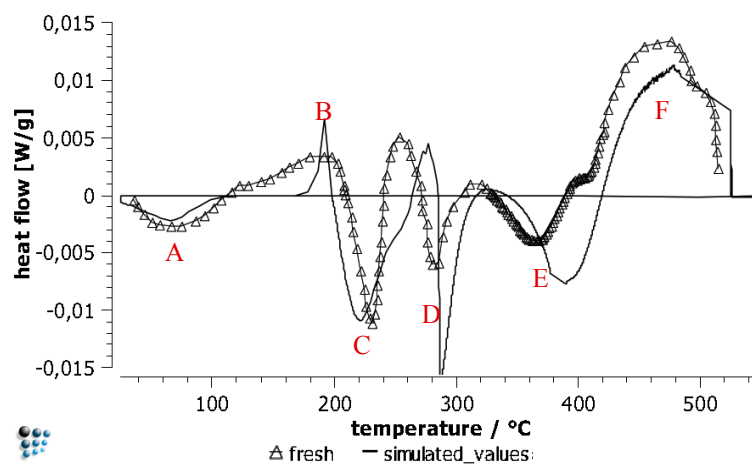


Fig. 2: Phase fraction of simulated metastable and stable phases with respect to temperature

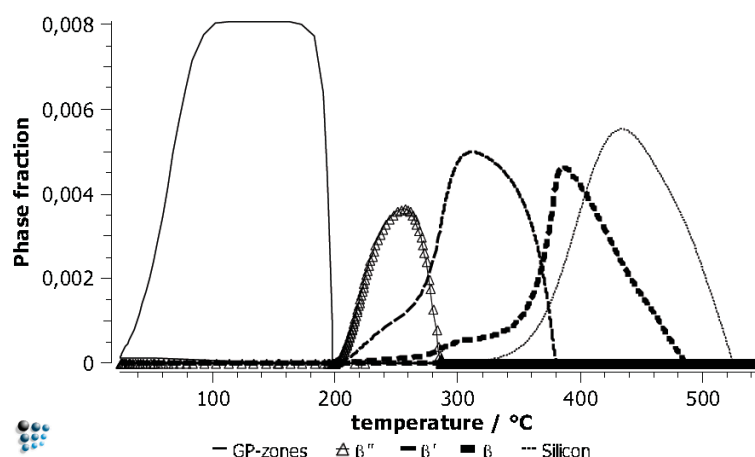


Fig. 2 shows the phase fraction of different metastable and stable phases in the material. The phase fraction of the GP-zones is relatively high compared to that of other phases. The phases have the same sequence of precipitation with respect to temperature as explained before, additionally including excess Si precipitation.

By looking at the predicted phase fractions (Fig. 2) and comparing them with corresponding DSC curves (Fig. 1), the interpretation of DSC curves will be given a new dimension. For example, the first descending part of peak D represents the dissolution of the β'' phase and at the same time precipitation of β' . The ascending part of the peak represents not only the precipitation of β' phase, but also a small amount of β phase precipitation. Overlapping of different exo- and endothermic peaks are involved in peak E, which is the result of the dissolution of the β' phase and at the same time the precipitation of β and Si. The ascending part of this peak partially involves dissolution of the β phase.

From the present investigation, we conclude that DSC curves alone can serve just as a rough indicator for precipitation and dissolution of phases and cannot be judged accurately unless suitable experimental methods are used to verify precipitates at each specific point [16]. This is very time consuming and expensive, however. Appropriate simulations can aid substantially to verify the assumed precipitation sequences and the interpretation of the DSC data.

5. Conclusion

In the present work, a combined assessment of available stereochemical information and first principles results of the metastable phases of the Al-Mg-Si system, self-diffusion data of Al and tracer diffusivities of Mg and Si in Al, as well as experimental DSC signals of both continuous heating and isothermal experiments thermodynamic descriptions of the metastable precipitates GP-zones, β'' , and β' has been carried out. With this strategy, and using the MatCalc software, optimized thermodynamic and kinetic model parameters are obtained. In our approach, the effect of quenched in vacancies, dislocation density of matrix and lattice mismatch effect of precipitates with matrix are included. From the simulations, it is possible to distinguish the precipitation behavior of the different metastable phases. Furthermore, quantitative predictions of important microstructural properties, such as number densities of precipitates and particle sizes, can be made. These results can be used for simulation of DSC curves in similar materials, as well as for calculations of yield strength as a function of aging time and temperature by any arbitrary heat treatment.

Acknowledgments

The authors acknowledge the provision of samples by Leichtmetall-Kompetenzzentrum Ranshofen/Austria and AMAG /Austria.

References

- [1] D.J. Chakrabarti, David E. Laughlin: Prog. Mater Sci. 49 (2004) 389–410.
- [2] M.A van Huis, J.H.Chen, M.H.F. Sluiter, H.W. Zandbergen: Acta Mater 55 (2007) 2183–2199.
- [3] N. Saunders, A.P.Miodownik: *CALPHAD (Calculation of Phase Diagrams): A Comprehensive Guide* (Pergamon Materials Series). Vol. 1. 1998.
- [4] J. Svoboda, F.D.Fischer, P. Fratzl, E. Kozeschnik: Mater. Sci. Eng. A 385 (2004) 166–174.
- [5] E. Povoden-Karadeniz, P. Warczok, P. Lang, A. Falahati, E. Kozeschnik: *unpublished research*. 2010.
- [6] A. Falahati, E. Povoden-Karadeniz, P. Lang, P. Warczok, E. Kozeschnik: *unpublished research*. 2010.
- [7] <http://www.matcalc.at>.
- [8] K. G. F. Janssens, D.Raabe, E. Kozeschnik, M. A. Miodownik, B. Nestler: *Computational materials engineering*, (Elsevier academic press 2007) P 153.
- [9] J.Svoboda, I. Turek, F.D. Fischer: Philos. Mag. 85 (2005) 3699–3707.
- [10] B. Sonderegger, E. Kozeschnik: Met. Trans. 40A (2009) 499-510.
- [11] F.D. Fischer, J.S., E. Gamsjäger, E. Kozeschnik, B. Sonderegger: Mater. Res. Soc. Symp Proc. 979 (2007) 0979-HH11-04.
- [12] M. Murayama, K. Hono: Acta Mater. 47 (1999) 1537-1548.
- [13] R. Vissers, M.A. van Huis, J. Jansen, H.W. Zandbergen, C.D. Marioara, S.J. Andersen Acta Mater 55 (2007) 3815–3823.
- [14] E. Hornbogen, A.K. Mukhopadhyay, E. A. Starke: Journal of Mater. Sci. 28 (1993) 3670-3674.
- [15] C. D. Marioara, S. J. Andersen, J. Jansen, H. W. Zandbergen: Acta Mater. 49 (2001) 321–328.
- [16] K. Matsuda, S. Ikeno, H. Matsui, T. Sato, K. Terayama, Y. Uetani: Metallurgical and Mat. Trans. 36 A (2005) 2007-2012.